Transplantation of human fetal blood stem cells in the osteogenesis imperfecta mouse leads to improvement in multiscale tissue properties

Maximilien Vanleene,[1] Zahraa Saldanha,[2] Kristy L. Cloyd,[3] Gavin Jell,[3] George Bou-Gharios,[4] J. H. Duncan Bassett,[5] Graham R. Williams,[5] Nicholas M. Fisk,[6] Michelle L. Oyen,[7] Molly M. Stevens,[3,8] *Pascale V. Guillot,[2] and *Sandra J. Shefelbine[1]

[1]Department of Bioengineering, [2]Institute of Reproductive and Developmental Biology, [3]Department of Materials, [4]Kennedy Institute of Rheumatology, and [5]Molecular Endocrinology Group, Department of Medicine & MRC Clinical Sciences Centre, Imperial College, London, United Kingdom; [6]University of Queensland, UQ Centre for Clinical Research, Brisbane, Queensland, Australia; [7]Department of Engineering, University of Cambridge, Cambridge, United Kingdom; and [8]Institute of Biomedical Engineering, Imperial College, London, United Kingdom

Osteogenesis imperfecta (OI or brittle bone disease) is a disorder of connective tissues caused by mutations in the collagen genes. We previously showed that intrauterine transplantation of human blood fetal stem/stromal cells in OI mice (*oim*) resulted in a significant reduction of bone fracture. This work examines the cellular mechanisms and mechanical bone modifications underlying these therapeutic effects, particularly examining the direct effects of donor collagen expression on bone material properties. In this study, we found an 84% reduction in femoral fractures in transplanted *oim* mice. Fetal blood stem/stromal cells engrafted in bones, differentiated into mature osteoblasts, expressed osteocalcin, and produced COL1a2 protein, which is absent in *oim* mice. The presence of normal collagen decreased hydroxyproline content in bones, altered the apatite crystal structure, increased the bone matrix stiffness, and reduced bone brittleness. In conclusion, expression of normal collagen from mature osteoblast of donor origin significantly decreased bone brittleness by improving the mechanical integrity of the bone at the molecular, tissue, and whole bone levels. (*Blood*. 2011;117(3):1053-1060)

Introduction

Osteogenesis imperfecta (OI) is a heterogeneous genetic disease with prenatal onset resulting from mutations within the collagen type 1 genes (*COL1a1* and *COL1a2*). OI is characterized by bone fragility, skeletal deformity, growth retardation, and in the severe forms, death.[1-4] Currently, no cure is available and pharmaceutical treatments only improve patients' symptoms through increases in bone density, failing to address the underlying bone brittleness and collagen defect. Stem cell therapy has the potential to replace defective osteoblasts with healthy ones that produce normal collagen. In humans, infusion of allogeneic whole bone marrow or bone marrow mesenchymal stem cells (MSCs) in children with OI led to increased bone mineral content, reduced fracture frequency, and improved growth velocity.[5-7] A single further clinical case used transplanted liver MSCs in utero combined with bisphosphonate therapy and noted better than expected progress in childhood.[8]

The *oim* mouse model (B6C3fe-a/a-col1a2^{oim}) shows biochemical and phenotypic features of human OI with reduced bone strength, multiple fractures, and skeletal deformities resulting from a spontaneous *COL1a2* chain gene mutation, resulting in the absence of normal heterotrimeric collagen COL1(a1)$_2$(a2)$_1$ and replacement by homotrimeric COL1(a1)$_3$. We have previously shown that intrauterine transplantation (IUT) of human first trimester fetal blood MSCs in *oim* mice resulted in a two-thirds reduction in long bone fracture incidence and improved mechanical and structural bone properties.[9] Donor cells were preferentially found at sites of bone remodeling (growth plate and fracture sites) where they differentiated into osteoblasts in vivo. Engraftment levels remained around 5%, and it was therefore unclear whether osteoblasts from donor origin only repaired de novo broken bones at fracture healing sites or also prevented fracture occurrence by directly contributing to amelioration of bone strength. Recently, Panaroni et al found that adult murine bone marrow transplanted in utero in the BrtlIV murine model of OI differentiated into collagen-producing osteoblasts, improving bone mechanical properties and eliminating the perinatal lethality of the BrtlIV mice despite low levels of engraftment.[10]

Altogether, these data suggest that donor cells may prevent bone pathology by direct differentiation and subsequent modifications in bone matrix composition, explaining why low levels of engraftment have been associated with pronounced therapeutic effects. To optimize stem cell therapy further, it is critical to understand how changes at the cellular level affect whole bone mechanics and fracture. In the present investigation, we examined the cellular mechanisms and multiscale bone mechanical, structural, and morphologic modifications underlying the therapeutic effects after IUT in *oim* mice of human fetal blood stem/stromal cells (fSCs), referred to elsewhere as MSCs.[9,11] We found an 84% decrease in femoral fracture incidence in *oim* mice after transplantation. Blood fSCs engrafted in bones and differentiated into mature osteoblasts that produced the COL1a2 chain protein absent in nontransplanted mice. The presence of normal collagen corresponded to a decrease in hydroxyproline content in bones, an improvement in mineral

Submitted May 28, 2010; accepted October 18, 2010. Prepublished online as *Blood* First Edition paper, November 18, 2010; DOI 10.1182/blood-2010-05-287565.

*P.V.G. and S.J.S. contributed equally to this study.

The online version of this article contains a data supplement.

The publication costs of this article were defrayed in part by page charge payment. Therefore, and solely to indicate this fact, this article is hereby marked "advertisement" in accordance with 18 USC section 1734.

structure, an increase in matrix stiffness, and a decrease in bone brittleness, which resulted in a decrease in fracture incidence in transplanted mice.

Methods

Blood fSC collection

Fetal blood collection received ethical approval from the Imperial College Institutional Review Board and the Home Office, as well as written informed consent from the pregnant women in accordance with the Declaration of Helsinki, as previously described.[9] Blood was collected by cardiocentesis under ultrasound guidance.[12] After selection by plastic adherence, fSCs (which we have previously referred to as fetal mesenchymal stem cells[9]) were cultured in Dulbecco modified Eagle medium-high glucose (Invitrogen) supplemented with 10% fetal bovine serum (BioSera), 100 IU/mL penicillin, and 100 μg/mL streptomycin (Invitrogen). Cells were expanded at 10 000 cells/cm^2 at 37°C with 5% CO_2.

oim mice breeding and fSC intrauterine transplantation

All experiments followed Home Office and institutional guidelines (Project license PPL 70/6852). Homozygous *oim/oim* mice (B6C3Fe-a/a-Col1a2^{oim}/Col1a2^{oim}) were bred from heterozygous *oim/+* mice (purchased from The Jackson Laboratory) and genotyped by direct sequencing of the *oim* fragment.[9] After mating of virgin *oim/oim* females with one *oim/oim* male, fetuses received intrauterine injection of fSCs (passages 3-6; cell quantity, 10^6 cells) at embryonic days (E) 13.5 to 15. Briefly, we performed a midline laparotomy on isoflurane-anesthetized females, and exteriorized the uterine horns one at a time, moisturized with warm phosphate-buffered saline. Each *oim* fetus received 10^6 cells injected intraperitoneally under direct vision using a 33-G Hamilton Microlitre syringe. Uterine horns were then replaced in the abdomen, and the wound was closed. Postoperatively, mice were given analgesia and individually housed in clean cages containing enrichment. After normal delivery, litters were kept with their mother until weaned at 4 to 6 weeks.

Animals

We analyzed 8-week-old wild type B6C3Fe-*a/a*-+/+ mice (WT, 8 females, 7 males), homozygous nontransplanted *oim*/*oim* mice (*oim*, 8 females, 12 males), and homozygous *oim*/*oim* mice transplanted with fSCs (*oim*+IUT, 5 females, 7 males). Hind limb bones were dissected, cleaned of soft tissue, and stored in PBS soaked gauze at −18°c. The number of femurs with a visible fracture callus was recorded; fractured femurs were not useable for 3-point bending and thus were not used in subsequent analysis.

Real-time quantitative RT-PCR

Total RNA was extracted from left femurs using TRIzol (Invitrogen) according to the manufacturer's instructions and cDNA synthesized using Pd(N)6 random hexamers (GE Healthcare). Real-time quantitative reverse transcriptase polymerase chain reaction (RT-PCR) was performed with the ABI Prism 7700 Sequence Detector (Applied Biosystems) according to the manufacturer's instructions, and all reactions were carried out in duplicate in a total volume of 25 μL. Human specific coding sequences from the β-actin gene (accession number NM_001101) were amplified in parallel with common human-mouse sequences to determine human-mouse microchimerism levels. The sequences of the PCR primers were described by Guillot et al.[9] Donor cell engraftment was expressed as human cells to total cells (human + mouse) percentage. Serial dilution of human cells with mouse cells formed the calibration curves by which chimerism was estimated.

Western blotting

Ground bone was added to 200 μL of 0.5M acetic acid (VWR International) and left at room temperature for 14 days to extract collagen from the bone tissue. Pepsin was then added to the sample at 0.264 mg/mL concentration. Supernatants were electrophoresed on a 6% sodium dodecyl sulfate-polyacrylamide gel electrophoresis gel (1 mm thickness, run at 150 V for 90 minutes). The gel was stained for 30 minutes in a staining solution of 0.1% Coomassie Brilliant Blue, 50% methanol, and 20% acetic acid, rinsed in destaining solution (30% methanol and 1% formic acid), and imaged. Human specific antibodies used were anticollagen (Sigma-Aldrich), followed by secondary antibody phosphatase-conjugated streptavidin (1:5000; Jackson ImmunoResearch Laboratories).

Hydroxyproline assay

Hydroxyproline levels were determined using the standard method described by Morrison et al.[13]

Raman spectroscopy

Twelve Raman spectra were recorded in the cortical bone of the right femurs (after macroscopic investigations): 3 spectra from anterior, posterior, lateral, and medial cross section quadrant. We analyzed 10 femurs per group (5 males and 5 females), using a Renishaw In Via system (Renishaw) equipped with a Renishaw spectrometer and a 785-nm diode laser (~ 100 mW at sample). Raman vibrational spectra were recorded from 400 to 1800 cm, allowing acquisition of peaks attributed to the bone matrix apatite crystals and proteins[14,15] (supplemental Figure 1, available on the *Blood* Web site; see the Supplemental Materials link at the top of the online article). Spectra were intensity and background corrected, smoothed, and normalized using custom MatLab programs.[16,17] Multivariate unsupervised principal component analysis of spectra determined combinations of variables (principal components [PCs]) that account for the major peak variation between spectra. Univariate spectral analyses were also performed to measure the area of 3 peaks: apatite υ_1 PO_4^{3-} peak (~ 960 cm), type B υ_1 CO_3^{2-} peak (~ 1070 cm), and amide I band (~ 1665 cm). Apatite mineral/protein matrix ratio (apatite $\upsilon_1PO_4^{3-}$/amide 1), which increases with bone mineral content,[15,18] was then assessed. Type B apatite carbonation (PO_4^{3-} ions substitution by CO_3^{2-} ions), which increases with maturation of mineralized matrix,[15] was calculated ($\upsilon_1CO_3^{2-}/\upsilon_1PO_4^{3-}$ peak area ratio). Apatite crystallinity was calculated as the inverse of the apatite $\upsilon_1PO_4^{3-}$ peak full width at half-maximal intensity. Crystallinity increases with apatite homogeneity and lattice orderliness (ie, improved mineral structure).[18]

Nanoindentation

Four intact tibiae per type group (2 males and 2 females) were dehydrated in alcohol baths and polymerized into low viscosity methyl methacrylate (VWR International). After transverse sectioning, tibial mid-diaphyseal cross sections were ground with carbide abrasive papers (P600 to P4000) and polished with 0.05 μm diamond suspension (Buehler). Sixty nanoindentation tests were performed around the tibia cross section at a maximum load of 8 mN and a constant loading/unloading rate: 800 μN/s, using a Berkovich diamond tip and a triboindenter TI700 UBI (supplemental Figure 2A-C). Time-depth unloading data were fitted with a viscous-elastic-plastic mathematical model[19,20] to determine the bone matrix plane-strain elastic modulus (E′), resistance to plastic deformation (H),[21] and indentation viscosity (η, Origin 8, Originlab; supplemental Figure 2D). The bone tissue compressive elastic modulus (E_{nano}) was calculated as $E' = E/(1 - \nu)^2$ with Poisson ratio $\upsilon = 0.3$.[22] Viscous deformation was negligible compared with elastic and plastic deformations (< 2% of total deformation) and was not considered further.

Femur bone morphology

Right femurs were scanned using a microcomputer tomography scanner (μCT40 Scanco Medical) with a 10-μm voxel resolution (45 kV, 177 μA, 200 ms integration time) and were analyzed using MicroView ABA 2.2 software (GE Healthcare). Cortical bone was analyzed at mid-diaphysis (1-mm-thick region of interest): cross-sectional area (CtA), mean thickness (CtTh), anterior-posterior (I_{ap}), and medial-lateral (I_{ml}) second moments of area. Distal metaphysis trabecular bone was also analyzed (75% to 87% of total femur length): trabecular thickness (TbTh) and spacing (TbSp), bone volume over total volume (BV/TV), and trabecular number (TbN).

Femur 3-point bending

After CT scanning, right femurs were tested until fracture by 3-point bending using a standard materials testing machine (5866 Instron). Femurs were loaded at the mid-diaphysis in the anterior-posterior direction with a deflection rate of 50 μm/s. Force-deflection curves were analyzed with a custom program (Matlab, MathWorks) to measure the bending stiffness (S, slope of the linear elastic deformation), the yield force (F_{yield}, limit between the elastic and plastic deformation), and ultimate force ($F_{ult,}$ maximum force sustained). The plastic (post-yield) behavior was assessed by the ratio of plastic/total work to fracture (Rp/tW, ie, ratio of the area under the curve from the yield point to the fracture point over the total area under the curve). The bone elastic modulus E (MPa) and ultimate stress σ_{ult} (MPa), were calculated using the standard beam theory.[13]

Statistical analysis

Statistical analyses were conducted with a 5% level of significance using SPSS 17.0. As *oim* mutation and MSC transplantation were found not sex dependent previously,[9,10,23,24] sex was pooled to maximize group size. Femur fracture occurrence was tested using a binomial test. Because of small sample size and unequal variance, morphology, bending, and Raman parameters were tested with multigroup Kruskal-Wallis followed by 2 × 2 Mann-Whitney (MW) tests (Bonferroni *P* value correction). Nanoindentation data were tested using analysis of variance (independent factor: group type, covariate: sex and specimen) followed by post-hoc Bonferroni test.

Results

IUT of blood fSCs led to a 84% reduction in femoral fractures

The number of femoral fracture calluses (indicating spontaneous bone fracture) was significantly reduced by 84% in transplanted *oim*+IUT mice compared with nontransplanted *oim* mice (binomial test, $P < .001$; ie, 4.2% in *oim*+IUT vs 27.5% in *oim* mice). In *oim* mice, 7 of 20 mice presented femurs with fracture calluses (4 mice with both femurs with callus were not included in the analyses). In *oim*+IUT mice, one of 12 mice presented one femur with fracture callus. No fracture calluses were observed in the WT group.

fSCs differentiated into mature osteoblasts producing COL1a2 chain protein

Donor cell engraftment in intact femurs (percentage of human donor cells over total number of cells) was low (median, 1.4%; range, 0.1%-16.2%, n = 12; supplemental Table 1) and consistent with our previous study.[9] Donor cells expressed markers of human derived mature osteoblasts (osteocalcin, 125-fold up-regulation), as well as proteins expressed at sites of mineralization (phosphatase 1, 24-fold up-regulation) and in condensing cartilage (noggin, 100-fold up-regulation) and other matrix proteins (bone morphogenetic protein-2, 128-fold up-regulation; bone sialoprotein, 24-fold up-regulation; and osteopontin, 30-fold up-regulation; Table 1). In WT animals, we did not detect these markers, as the primers were designed to be human specific. Western blot analysis showed the presence of the COL1a2 protein band in transplanted *oim*+IUT femurs, which was absent in nontransplanted *oim* femurs (Figure 1A). In line with this result, hydroxyproline, which has a higher content in COL1a1 than in COL1a2 chains,[25] was decreased in *oim*+IUT mice compared with *oim* mice (8.6 ± 1.1 μg/mg tissue, n = 11 vs 13.4 ± 0.7 μg/mg tissue, n = 15; MW test, $P < .001$; Figure 1B), suggesting that the COL1a2 chain of donor origin contributed to a decrease in endogenous COL1a1 content.

Table 1. Up-regulation of bone-specific markers using quantitative RT-PCR and human specific markers

	Naive ($2^{-}\Delta Ct$)	Transplanted ($2^{-}\Delta Ct$)	Fold increase
Osteocalcin	4.8×10^{-7}	5.9×10^{-5}	123.6
Phosphatase 1	4.0×10^{-5}	9.8×10^{-4}	24.3
Noggin	3.1×10^{-4}	3.1×10^{-2}	101.1
BMP2	3.1×10^{-5}	3.9×10^{-2}	128.0
BSP	2.0×10^{-5}	4.9×10^{-4}	24.3
Osteopontin	1.7×10^{-5}	5.1×10^{-2}	29.9

The differences in gene expression reported refer to the expression of the basal levels in undifferentiated human cells. BMP2 indicates bone morphogenetic protein-2; and BSP, bone sialoprotein.

Bone matrix composition

Raman spectroscopy was used to assess the biochemical composition fingerprint of cortical bone matrix. Principal component analysis is a multivariate statistical technique describing the overall variability among spectra through calculation of PCs. Instead of comparing each peak separately, this technique allows comparison of the entire spectra. The PCs are new variables, which account for the majority of variation between spectra and are composed of weighted contributions of the spectrum wave numbers (peaks). Results showed that WT and *oim* groups can be distinguished by the first principal component (PC1, Figure 2A horizontal axis). The weighting of the wave numbers that compose PC1 (Figure 2B) indicates that PC1 has contributions primarily because of the collagen protein peaks (at 1240, 1445, and 1665 cm^{1}) and the apatite peak (apatite $\upsilon_1 PO_4^{3-} \sim 960\ cm^{1}$). The principal component 2 (PC2) separated transplanted and nontransplanted *oim* mice, albeit only for the females (Figure 2C vertical axis). The weighting of the wave numbers that compose PC2 (Figure 2D) indicates that PC2 has contributions primarily from the mineral bands (apatite $\upsilon_1 PO_4^{3-}$: ~ 960 cm, type B carbonate $\upsilon_1 CO_3^{2-}$: 1070 cm^{-1}). This may indicate that fSC transplantation affects males and females differently.

Analysis of specific peaks in the Raman spectra (univariate analysis) allowed assessment of the bone mineral/protein ratio, the apatite crystal maturation, and apatite crystallinity. Analysis of the

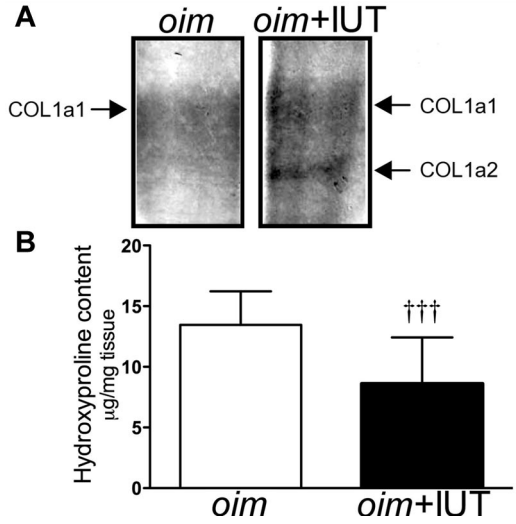

Figure 1. oim+IUT bones showed the presence of Col1a2 protein expressed by the donor cells. (A) Coomassie stain showing the presence of Col1a2 band in *oim*+IUT femurs. (B) Hydroxyproline content in *oim* and *oim*+IUT mice. †††$P < .001$ (Mann-Whitney test).

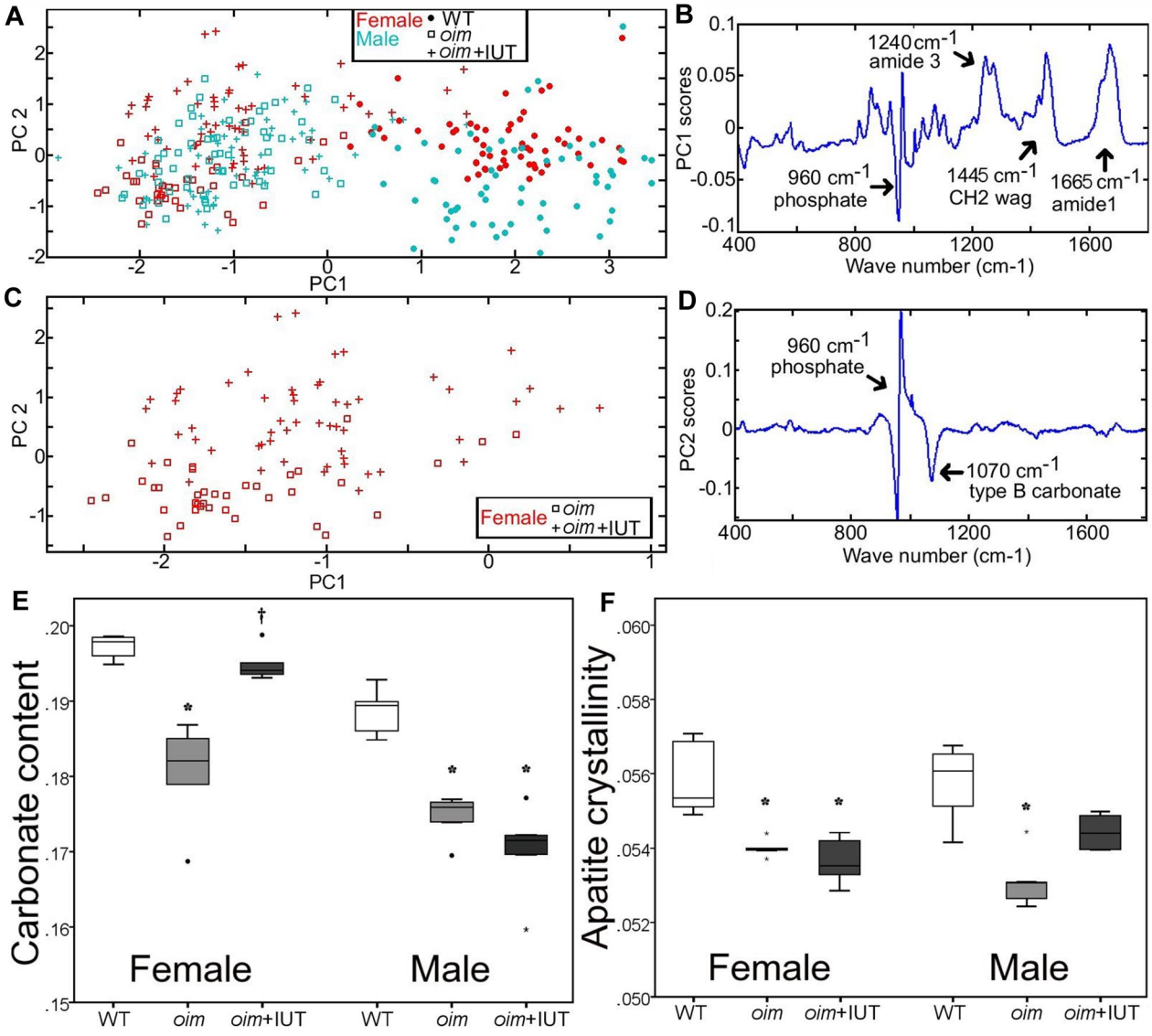

Figure 2. Raman spectroscopy analysis of the cortical bone tissue of WT, *oim*, and *oim*+IUT mice. (A) PC1 versus PC2 obtained demonstrates that PC1 differentiates WT from *oim* and *oim*+IUT. (B) Weighting of spectrum frequencies contributing to PC1. (C) Subset of data from panel A showing that female *oim* and *oim*+IUT are differentiated by PC2. (D) Weighting of spectrum frequencies contributing to PC2. (E) Carbonate content. (F) Apatite crystallinity obtained by univariate peak analysis of the Raman spectra. *$P < .05$ (significant difference vs WT group). †$P < .05$ (significant difference vs *oim* group).

groups pooling genders revealed significantly lower mineral/protein ratio and higher apatite crystal maturation, and crystallinity of WT mice compared with both *oim* groups (*oim* and *oim*+IUT) but no significant difference between *oim* and *oim*+IUT (supplemental Table 2). Because principle component analysis suggested a difference in genders (PC2 in particular), we also analyzed univariate parameters for male and female separately (supplemental Table 3). Female *oim*+IUT bone matrix exhibited a higher apatite maturation than *oim* mice (0.194 ± 0.002 vs 0.180 ± 0.008, respectively, $P < .05$) and was similar to WT (0.197 ± 0.001, $P > .05$), indicating that transplantation may increase the maturation of the bone mineralized matrix in the female group (Figure 2E). In males, apatite maturation was not significantly different between *oim* and *oim*+IUT ($P = 1.0$). In females, apatite crystallinity was not significantly different between *oim* and *oim*+IUT ($P = 1.0$), but in males exhibited a slight but not significant increase (p = .14; Figure 2F).

Transplantation increased bone matrix stiffness

Nanoindentation assessment found that *oim*+IUT mice exhibited a stiffer bone matrix than *oim* mice (larger E_{nano}, $P < .001$) but did not reach the stiffness of WT matrix (Figure 3A). Resistance to plastic deformation (H) did not differ between *oim* and *oim*+IUT groups ($P > .05$) and was higher than WT bone ($P < .001$ for both, Figure 3B).

Transplantation decreased bone brittleness

Mechanical strength of intact femurs was assessed using the 3-point bending test. Typical load-deflection curves obtained during tests are illustrated in Figure 4A. Analysis of load-deformation curves showed that F_{ult}, stiffness (S), and F_{yield} were not significantly different between *oim*+IUT and *oim* mice, indicating that femurs were not stronger after transplantation

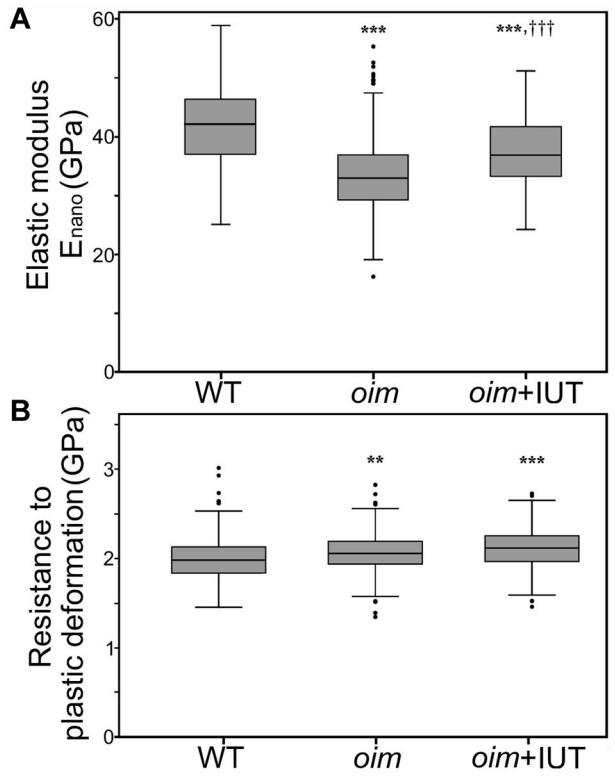

Figure 3. Microscopic scale mechanical properties. (A) Nanoindentation revealed an increase in elastic modulus in the *oim*+IUT bones compared with *oim*. (B) Resistance to plastic deformation was unchanged in *oim*+IUT bones compared with *oim* (analysis of variance test and Bonferroni post-hoc tests). $^{**}P < .01$ (significant difference vs WT group). $^{***}P < .001$ (significant difference vs WT group). $\dagger\dagger\dagger P < .001$ (significant difference vs *oim* group). Box and whisker plots represent the group median and quartiles (box) and 1.5× interquartile distance (whiskers). Round symbols represent outliers, which exceed the whiskers values.

(Table 2). However, the Rp/tW, which describes the femur postyield behavior (plastic deformation, crack formation and propagation, and ultimately fractures) had a nearly 2-fold increase for *oim*+IUT bones compared with *oim* bones (*oim*+IUT: 63.9% ± 21.9% vs *oim*: 33.6% ± 25.8%, $P < .01$), indicating that transplanted bones had more plastic deformation, required more work to fracture, and had decreased brittleness compared with nontransplanted *oim* bones (Figure 4B). Macroscopic bone material properties were derived from 3-point bending tests using the classic beam bending analysis. Bone elastic moduli (E) were similar among the 3 groups ($P > .05$). Ultimate stress (σ_{ult}) of the *oim*+IUT mice was not significantly different from WT and *oim* group ($P > .05$ for both), but WT bones were significantly stronger than both *oim* and *oim*+IUT ($P < .01$).

No changes in bone morphology

Micro-CT images revealed no significant difference of cortical bone morphology in CtTh, CtA, and second moments of inertia (I_{ap}, I_{ml}) between *oim* + IUT and *oim* mice ($P > .05$; Table 3). Compared with WT femurs, both *oim* and *oim*+IUT femurs exhibited thinner cortical bone, smaller CtA, and reduced second moments of area (for *oim*+IUT, $P < .001$ for all parameters, for *oim*, $P = .114$, $P = .048$, $P = .001$, and $P < .001$ for CtTh, CtA, I_{ap}, and I_{ml}, respectively). Trabecular bone morphology (BV/TV, TbSp, TbN) did not differ between *oim* + IUT and *oim* mice ($P > .05$ for all parameter). Compared with WT mice, *oim* and *oim*+IUT mice had lower BV/TV, with reduced TbN and increased TbSp ($P < .001$ for all parameters for both groups). Trabecular thickness did not vary among the groups ($P > .05$).

Discussion

In utero transplantation of human fetal blood stem/stromal cells in homozygous *oim* mice led to an 84% reduction of femur fracture incidence, albeit associated with a less than 5% donor cell engraftment rate. These results are consistent with our previous study using the same cell type[9] and raise the possibility that therapeutic changes may be mediated by paracrine effects as is found in other MSC transplantation paradigms[26-29] rather than direct differentiation. Here, we investigated whether donor cells were directly contributing to the phenotypical improvements associated with transplantation by analyzing biochemical, structural, and mechanical properties of the bone. We found that differentiation of donor fSCs into mature osteoblasts produced the missing protein COL1a2, modified the composition of the bone matrix, increased the stiffness of the matrix, and rendered the bones less brittle and less prone to fracture.

The dramatic decrease in fractures may be explained at the macroscopic scale by a reduction of bone brittleness rather than by an increase in strength. In previous work, an increase of bending strength was found in tibiae but not in humeri (femurs were not tested).[9] In this study, we found no change in bending strength in

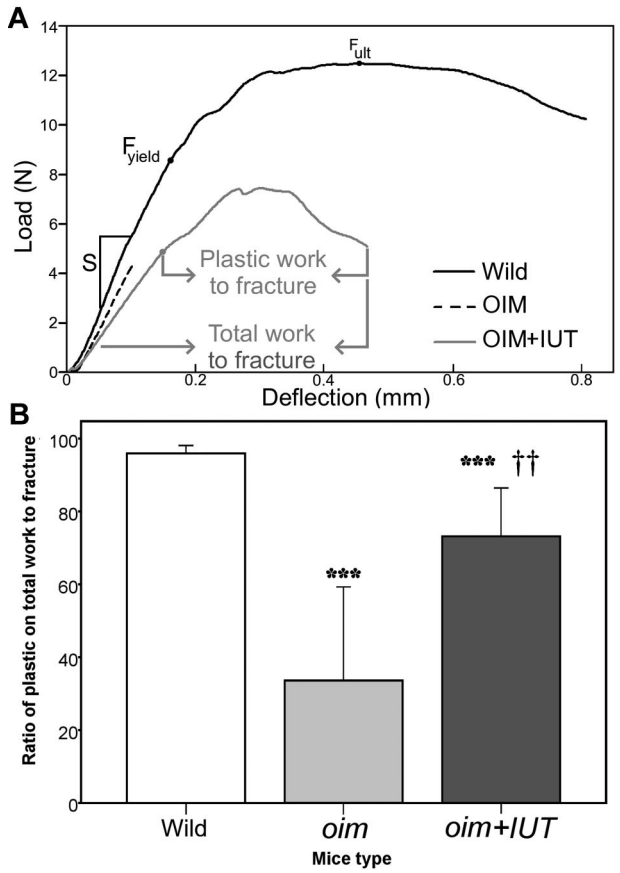

Figure 4. Three-point bending mechanical testing. (A) Representative examples of 3-point bending load-deflection curves until fracture obtained for WT, *oim*, and *oim*+IUT femurs: stiffness (S), ultimate force (F_{ult}), yield force (F_{yield}), and total and plastic work to fracture are indicated. (B) Box-plot of the ratio of plastic/total work to fracture. $^{***}P < .001$ (significant difference vs WT group). $\dagger\dagger P < .01$ (significant difference vs *oim* group).

Table 2. Mechanical properties of WT, *oim*, and *oim* + IUT femurs measured from 3-point bending load-displacement curves

	Macroscopic scale mechanical properties					
	WT (n = 15)	*oim* (n = 15)	*P**	*oim*+IUT (n = 11)	*P**	*P*†
F_{ult}, N	12.4 ± 2.4; 11.8	6.1 ± 2.8; 6.4	< .001	6.0 ± 2.1; 6.3	< .001	NS
S, N/mm	69.4 ± 11.4; 70.2	41.3 ± 16.4; 42.3	< .001	35.5 ± 10.4; 38.2	< .001	NS
F_{yield}, N	6.8 ± 1.6; 6.1	5.2 ± 2.6; 4.6	NS	4.2 ± 1.4; 4.4	< .001	NS
Rp/tW, %	95.9 ± 2.2; 96.2	33.6 ± 25.8; 29.5	< .001	63.9 ± 21.9; 65.1	< .001	.002
σ_{ult}, MPa	123.0 ± 8.6; 124.5	90.0 ± 34.6; 97.1	.005	106.5 ± 49.0; 94.2	NS	NS
E, MPa	6935.9 ± 748.9; 7229.4	6996.0 ± 1175.1; 7138.2	NS	7363.4 ± 3180.2; 7159.2	NS	NS

Data are mean plus or minus SD; median.
NS indicates no significant difference.
*Test versus WT group (Mann-Whitney test).
†Test versus *oim* group (Mann-Whitney test).

the femur. This discrepancy may highlight a variation in therapy efficiency at different bone sites and will be examined more closely in future studies. In this study, 4 of our 20 *oim* mice had fracture callus on both femurs and were excluded (because mechanical testing required intact femurs), which have necessarily biased the *oim* group toward the strongest bone of the *oim* phenotype and may have underestimated differences between *oim* and *oim* + IUT mice.

We found no effect of transplantation in femoral bone morphology (cortical and trabecular), indicating that the reduction of fracture rate cannot be attributed to a change of femur shape or size but rather to a change of bone tissue properties. Calculating macroscopic bone tissue properties from 3-point bending data, we found no differences among groups. However, these calculations require material and geometry approximations of the sample[30,31] and therefore give only rough estimates. Previous studies of *oim* bone using similar bending protocols have found a broad range of tissue properties, indicating that this technique may not appropriately detect minor changes in tissue modulus,[23,24] thus necessitating the use of nanoindentation.

At the bone matrix scale, nanoindentation revealed a significant increase in elastic modulus in *oim*+IUT bones despite the large heterogeneity of microscopic material properties within a single specimen, which is fairly characteristic of normal bone.[32,33] We investigated whether the changes in matrix mechanical properties resulted from alterations in the protein-mineral structure at the molecular level. Raman spectroscopy analyses exhibited a trend toward more mature apatite crystal (more carbonated apatite), which seemed to be more pronounced in the female group.

Such sex difference has not previously been reported in stem cell therapies for OI. Influences of donor cell sex have been observed in cardiovascular stem cell therapies[34-37] and may suggest an effect of estrogens on stem cell activities. In vitro it has been shown that estrogen affects male and female bone marrow MSCs differently.[38,39] Other studies have found differences in male and female stem cell characteristics in skeletal tissue regeneration both in vitro[40] and in vivo.[41] Considering that our study was not designed to examine gender differences after IUT (and was underpowered to do so), it is difficult to deduce the effects of gender on the effectiveness of stem cell therapy (all donor cells were female in this study). However, these intriguing differences warrant further study.

Our results suggest that the presence of normal collagen after human blood fSC transplantation influenced apatite crystal structure, which is in accordance with Panaroni et al who found improvement in crystal homogeneity after IUT of adult mouse bone marrow in the BrtlIV murine OI model.[10] Similarly, heterozygous *oim*/+ mice, expressing both normal and abnormal collagen, exhibit increased apatite carbonate content (more mature crystals)[42,43] and larger and more organized apatite crystals compared with homozygous *oim* mice.[44,45] Altogether, these data indicate that the presence (or absence) of normal collagen may affect bone mineral structure.

An increase in mineral content in healthy human and animal bone tissue normally corresponds to an increase in bone matrix stiffness.[46,47] In contrast, we found increased mineral content in *oim* and *oim* + IUT compared with WT mice but lower matrix stiffness. Similar to other nanoindentation studies of bone, our results showed a large heterogeneity of microscopic material properties within a single specimen.[32,48] We thoroughly sampled 4 specimens (60 indents/bone) from each group (rather than only a few indents from every bone). Therefore, the specimens tested may not fully

Table 3. Cortical and trabecular morphologic parameters measured from WT, oim, and *oim* + IUT femurs

	Bone morphology parameters					
	WT (n = 15)	*oim* (n = 16)	*P**	*oim*+IUT (n = 12)	*P**	*P*†
Cortical bone						
CtTh, mm	0.211 ± 0.024; 0.207	0.183 ± 0.034; 0.184	NS	0.164 ± 0.020; 0.164	< .001	NS
CtA, mm^2	0.863 ± 0.130; 0.835	0.678 ± 0.185; 0.674	.048	0.584 ± 0.077; 0.591	< .001	NS
I_{ap}, mm^4	0.261 ± 0.079; 0.231	0.152 ± 0.062; 0.148	.001	0.118 ± 0.024; 0.118	< .001	NS
I_{ml}, mm^4	0.157 ± 0.039; 0.141	0.090 ± 0.037; 0.085	< .001	0.072 ± 0.017; 0.068	< .001	NS
Trabecular bone						
TbTh, mm	0.041 ± 0.002; 0.041	0.041 ± 0.003; 0.040	NS	0.043 ± 0.007; 0.041	NS	NS
TbSp, mm	0.121 ± 0.019; 0.126	0.201 ± 0.036; 0.207	< .001	0.230 ± 0.049; 0.224	< .001	NS
BV/TV	0.243 ± 0.049; 0.234	0.126 ± 0.032; 0.119	< .001	0.102 ± 0.033; 0.104	< .001	NS
TbN, mm	6.1 ± 0.9; 6.0	3.3 ± 0.7; 3.2	< .001	3.1 ± 1.1; 2.9	< .001	NS

Data are mean plus or minus SD; median.
NS indicates no significant difference.
*Test versus WT group (Mann-Whitney test).
†Test versus *oim* group (Mann-Whitney test).

represent the intergroup heterogeneity but were nonetheless able to detect an increase in stiffness in *oim*+IUT mice. This stiffness increase is probably the result of the disorganization of the collagen fibers in *oim* bone, which provide a poor template for crystal organization and a reduction of mechanical integrity.[44,45,49] The relative improvement of matrix stiffness after transplantation is probably attributed to the addition of COL1a2 chain to the collagen protein, allowing a more organized and structured collagen-apatite crystal matrix.

In addition to improvement in matrix stiffness, we suspect there is also an improvement in the bone tissue organization that plays a significant role in improving the fracture toughness observed at the macroscopic scale. Organized lamellar bone was observed in larger amounts in treated bones compared with nontreated femur bone specimens from our previous investigation (data not shown). Studies have shown that the lamellar bone structure is critical for deterring crack propagation and dissipating energy during failure in WT mice and that disruption of this lamellar structure can lead to faster crack propagation and failure.[50,51] This hypothesis will be pursued in future research.

Altogether, our study indicated that fSCs transplanted in utero in *oim* mice migrated to bone, differentiated into mature osteoblasts, and expressed the missing protein COL1a2, altering the apatite mineral structure and increasing bone matrix stiffness. The changes in microscopic material properties and microarchitecture contribute to the mechanical integrity of the bone, making the bone less brittle and resulting in a decreased incidence of fracture. Further work will investigate strategies to maximize donor cell homing to bone, differentiation, and collagen expression to maximize the therapeutic effects of transplantation.

Acknowledgments

This work was supported by the British Birth Defect Foundation (S.J.S., P.V.G., and N.M.F.) and the Institute of Obstetrics & Gynaecology Trust (P.V.G. and N.M.F.). P.V.G. and S.J.S. were supported by Research Councils United Kingdom.

Authorship

Contribution: M.V., P.V.G., and S.J.S. conceived the experiments; P.V.G. performed stem cell transplantation; M.V., P.V.G., Z.S., and G.B.-G. performed experiments; M.V., K.L.C., G.J., and M.M.S. performed Raman analysis; M.L.O. performed nanoindentation analysis; M.V., S.J.S., and P.V.G. wrote the paper; and M.M.S., J.H.D.B., G.R.W., and N.M.F. revised the manuscript.

Conflict-of-interest disclosure: The authors declare no competing financial interests.

Correspondence: Sandra J. Shefelbine, Department of Bioengineering, Imperial College London, South Kensington Campus, Exhibition Rd, London, SW7 2AZ, United Kingdom; e-mail: s.shefelbine@imperial.ac.uk; and Pascale V. Guillot, Institute of Reproductive and Developmental Biology, Imperial College London, Hammersmith Campus, Du Cane Rd, London W12 0NN, United Kingdom; e-mail: Pascale.Guillot@imperial.ac.uk.

References

1. Glorieux FH. Osteogenesis imperfecta. *Best Pract Res Clin Rheumatol.* 2008;22(1):85-100.
2. Millington-Ward S, McMahon HP, Farrar GJ. Emerging therapeutic approaches for osteogenesis imperfecta. *Trends Mol Med.* 2005;11(6):299-305.
3. Rauch F, Glorieux FH. Osteogenesis imperfecta. *Lancet.* 2004;363(9418):1377-1385.
4. Rauch F, Glorieux FH. Osteogenesis imperfecta, current and future medical treatment. *Am J Med Genet C.* 2005;139C:31-37.
5. Horwitz EM, Prockop DJ, Fitzpatrick LA, Koo WWK. Transplantability and therapeutic effects of bone marrow-derived mesenchymal cells in children with osteogenesis imperfecta. *Nat Med.* 1999;5:309-313.
6. Horwitz EM, Prockop DJ, Gordon PL, et al. Clinical responses to bone marrow transplantation in children with severe osteogenesis imperfecta. *Blood.* 2001;97(5):1227.
7. Horwitz EM, Gordon PL, Koo WKK, et al. Isolated allogeneic bone marrow-derived mesenchymal cells engraft and stimulate growth in children with osteogenesis imperfecta: implications for cell therapy of bone. *Proc Natl Acad Sci U S A.* 2002;99(13):8932-8937.
8. Le Blanc K, Götherström C, Ringdén O, et al. Fetal mesenchymal stem-cell engraftment in bone after in utero transplantation in a patient with severe osteogenesis imperfecta. *Transplantation.* 2005;79(11):1607-1614.
9. Guillot PV, Abass O, Bassett JH, et al. Intrauterine transplantation of human fetal mesenchymal stem cells from first-trimester blood repairs bone and reduces fractures in osteogenesis imperfecta mice. *Blood.* 2008;111(3):1717-1725.
10. Panaroni C, Gioia R, Lupi A, et al. In utero transplantation of adult bone marrow decreases perinatal lethality and rescues the bone phenotype in the knockin murine model for classical, dominant osteogenesis imperfecta. *Blood.* 2009;114(2):459-468.
11. Guillot PV, Gotherstrom C, Chan J, Kurata H, Fisk NM. Human first trimester fetal mesenchymal stem cells (MSC) express pluripotency markers, grow faster and have longer telomeres compared to adult MSC. *Stem Cells.* 2007;25(3):646-654.
12. Campagnoli C, Roberts IA, Kumar S, Bennett PR, Bellantuono I, Fisk NM. Identification of mesenchymal stem/progenitor cells in human first-trimester fetal blood, liver, and bone marrow. *Blood.* 2001;98:2396-2402.
13. Morrison J, Palmer DB, Cobbold S, Partridge T, Bou-Gharios G. Effects of T-lymphocyte depletion on muscle fibrosis in the mdx mouse *Am J Pathol.* 2005;166:1701-1710.
14. Penel G, Leroy G, Rey C, Bres E. Micro Raman spectral study of the PO4 and CO3 vibrational modes in synthetic and biological apatites. *Calcif Tissue Int.* 1998;63(6):475-481.
15. Tarnowski CP, Ignelzi MA, Morris MD. Mineralization of developing mouse calvaria as revealed by Raman microspectroscopy. *J Bone Miner Res.* 2002;17(6):1118-1126.
16. Swain RJ, Jell G, Stevens MM. Non-invasive analysis of cell cycle dynamics in single living cells with Raman micro-spectroscopy. *J Cell Biochem Suppl.* 2008;104:1427-1438.
17. Gentleman E, Swain RJ, Evans ND, et al. Comparative materials differences revealed in engineered bone as a function of cell-specific differentiation. *Nat Mater.* 2009;8:763-770.
18. Akkus O, Adar F, Schaffler MB. Age-related changes in physicochemical properties of mineral crystals are related to impaired mechanical function of cortical bone. *Bone.* 2004;34:443-453.
19. Oyen ML, Ko C-C. Examination of local variations in viscous, elastic, and plastic indentation responses in healing bone. *J Mater Sci Mater Med.* 2007;18(4):623-628.
20. Oyen ML, Cook RF. Load-displacement behaviour during sharp indentation of viscous-elastic-plastic materials. *J Mater Res.* 2003;18(1):139-150.
21. Oyen ML. Nanoindentation hardness of mineralized tissues. *J Biomech.* 2006;39(14):2699.
22. Rho JY, Zioupos P, Currey JD, Pharr GM. Variation in the individual thick lamellar properties within osteons by nanoindentation. *Bone.* 1999;25:295-300.
23. McCarthy EA, Raggio CL, Hossack MD, et al. Alendronate treatment for infants with osteogenesis imperfecta: demonstration of efficacy in a mouse model. *Pediatr Res.* 2002;52(5):660-670.
24. Misof BM, Roschger P, Baldini T, et al. Differential effects of alendronate treatment on bone from growing osteogenesis imperfecta and wild-type mouse. *Bone.* 2005;36(1):150-158.
25. Miles CA, Sims TJ, Camacho NP, Bailey AJ. The role of the [alpha]2 chain in the stabilization of the collagen type I heterotrimer: a study of the type I homotrimer in oim mouse tissues. *J Mol Biol.* 2002;321(5):797-805.
26. Aslam M, Baveja R, Liang OD, et al. Bone marrow stromal cells attenuate lung injury in a murine model of neonatal chronic lung disease. *Am J Respir Crit Care Med.* 2009;180(11):1122-1130.
27. Baer PC, Geiger H. Mesenchymal stem cell interactions with growth factors on kidney repair. *Curr Opin Nephrol Hypertens.* 2010;19(1):1-6.
28. Laurila JP, Laatikainen L, Castellone MD, et al. Human embryonic stem cell-derived mesenchymal stromal cell transplantation in a rat hind limb injury model *Cytotherapy.* 2009;11(6):726-737.
29. Xu R-X, Chen X, Chen J-H, Han Y, Han B-M. Mesenchymal stem cells promote cardiomyocyte hypertrophy in vitro through hypoxia-induced aracrine mechanisms. *Clin Exp Pharmacol Physiol.* 2009;36(2):176-180.
30. Schriefer JL, Robling AG, Warden SJ, Fournier

AJ, Mason JJ, Turner CH. A comparison of mechanical properties derived from multiple skeletal sites in mice. *J Biomech.* 2005;38(3):467-475.

31. van Lenthe GH, Voide R, Boyd SK, Müller R. Tissue modulus calculated from beam theory is biased by bone size and geometry: implications for the use of three-point bending tests to determine bone tissue modulus. *Bone.* 2008;43(4):717-723.
32. Guo XE, Goldstein SA. Vertebral trabecular bone microscopic tissue elastic modulus and hardness do not change in ovariectomized rats. *J Orthop Res.* 2000;18:333-336.
33. Hengsberger S, Boivin G, Zysset PK. Morphological and mechanical properties of bone structural units: a two-case study. *JSME Int J.* 2002;454(4): 936-943.
34. Crisostomo PR, Markel TA, Wang M, Lahm T, Lillemoe KD, Meldrum DR. In the adult mesenchymal stem cell population, source gender is a biologically relevant aspect of protective power. *Surgery.* 2007;142(2):215-221.
35. Deasy BM, Lu A, Tebbets JC, et al. A role for cell sex in stem cell-mediated skeletal muscle regeneration: female cells have higher muscle regeneration efficiency. *J Cell Biol.* 2007;177(1):73-86.
36. Ray R, Novotny NM, Crisostomo PR, Lahm T, Abarbanell A, Meldrum DR. Sex steroids and stem cell function. *Mol Med.* 2008;14(7):493-501.
37. Herrmann JL, Abarbanell AM, Weil BB, et al. Gender dimorphism in progenitor and stem cell function in cardiovascular disease. *J Cardiovasc Transl Res.* 2010;3:103-113.
38. Hong L, Sultana H, Paulius K, Zhang G. Steroid regulation of proliferation and osteogenic differentiation of bone marrow stromal cells: a gender difference. *J Steroid Biochem Mol Biol.* 2009;114: 180-185.
39. Hong L, Zhang G, Sultana H, Yu Y, Wei Z. The effects of 17-β estradiol on enhancing proliferation of human bone marrow mesenchymal stromal cells in vitro. *Stem Cells Dev.* 2010 Oct 17 [Epub ahead of print[rsqsb].
40. Corsi KA, Pollett JB, Phillippi JA, Usas A, Li G, Huard J. Osteogenic potential of postnatal skeletal muscle-derived stem cells is influenced by donor sex. *J Bone Miner Res.* 2007;22(10):1592-1602.
41. Strube P, Mehta SS, Baerenwaldt A, et al. Sex-specific compromised bone healing in female rats might be associated with a decrease of stem cell quantity. *Bone.* 2009;45:1065-1072.
42. Camacho NP, Landis WJ, Boskey AL. Mineral changes in a mouse model of osteogenesis imperfecta detected by Fourier transform infrared microscopy. *Connect Tissue Res.* 1996;35(1): 259-265.
43. Camacho NP, Hou L, Toledano TR, et al. The material basis for reduced mechanical properties in oim mice bones. *J Bone Miner Res.* 1999;14(2): 264-272.
44. Fratzl P, Paris O, Klaushofer K, Landis WJ. Bone mineralization in an osteogenesis imperfecta mouse model studied by small-angle x-ray scattering. *J Clin Invest.* 1996;97(2):396-402.
45. Grabner B, Landis WJ, Roschger P, et al. Age- and genotype-dependence of bone material properties in the osteogenesis imperfecta murine model (oim). *Bone.* 2001;29(5):453-457.
46. Hoc T, Henry L, Verdier M, Aubry D, Sedel L, Meunier A. Effect of the microstructure on the mechanical properties of haversian cortical bone. *Bone.* 2006;38:466-474.
47. Huja SS, Beck FM, Thurman DT. Indentation properties of young and old osteons. *Calcif Tissue Int.* 2006;78(6):392-397.
48. Hengsberger S, Kulik A, Zysset P. Nanoindentation discriminates the elastic properties of individual human bone lamellae under dry and physiological condition. *Bone.* 2002;30(1):178-184.
49. Vetter U, Eanes ED, Kopp JB, Termine JD, Gehron Robey P. Changes in apatite crystal size in bones of patients with osteogenesis imperfecta. *Calcif Tissue Int.* 1991;49:248-250.
50. Jepsen KJ, Goldstein SA, Kuhn JL, Schaffler MB, Bonadio J. Type 1 collagen mutation compromises the post-yield behavior of Mov13 long bone. *J Orthop Res.* 1996;14(3):493-499.
51. Jepsen KJ, Schaffler MB, Kuhn JL, Goulet RW, Bonadio J, Goldstein SA. Type 1 collagen mutation alters the strength and fatigue behavior of Mov13 cortical tissue. *J Biomech.* 1997;30(11): 1141-1147.